



INFLUENCE OF ANNEALING TEMPERATURE ON DEGRADATION EFFICIENCY AND IRON OXIDE TRANSFORMATIONS IN CeO₂/Fe-OXIDE SORBENTS

O. Životský,¹ J. Luňáček,¹ Y. Jirásková,² J. Buršík,² J. Ederer,³ P. Janoš,³ K. Čabanová⁴

¹ VŠB-Technical University of Ostrava, Department of Physics, Ostrava, Czech Republic, ondrej.zivotsky@vsb.cz, jiri.lunacek@vsb.cz

² CEITEC IPM, Institute of Physics of Materials, AS CR, Brno, Czech Republic, jirasko@ipm.cz

³ Faculty of the Environment, University of Jan Evangelista Purkyně, Ústí nad Labem, Czech Republic, jakub.ederer@ujep.cz, pavel.janos@ujep.cz

⁴ VŠB – Technical University of Ostrava, Centre of Advanced Innovation Technologies, Ostrava, Czech Republic, kristina.cabanova@vsb.cz

AIM: Preparation, microstructural, and physical characterization of magnetically separable CeO₂(5 wt.%)/Fe-oxide powder sorbents with a demonstration of degradation capabilities against selected pesticides.

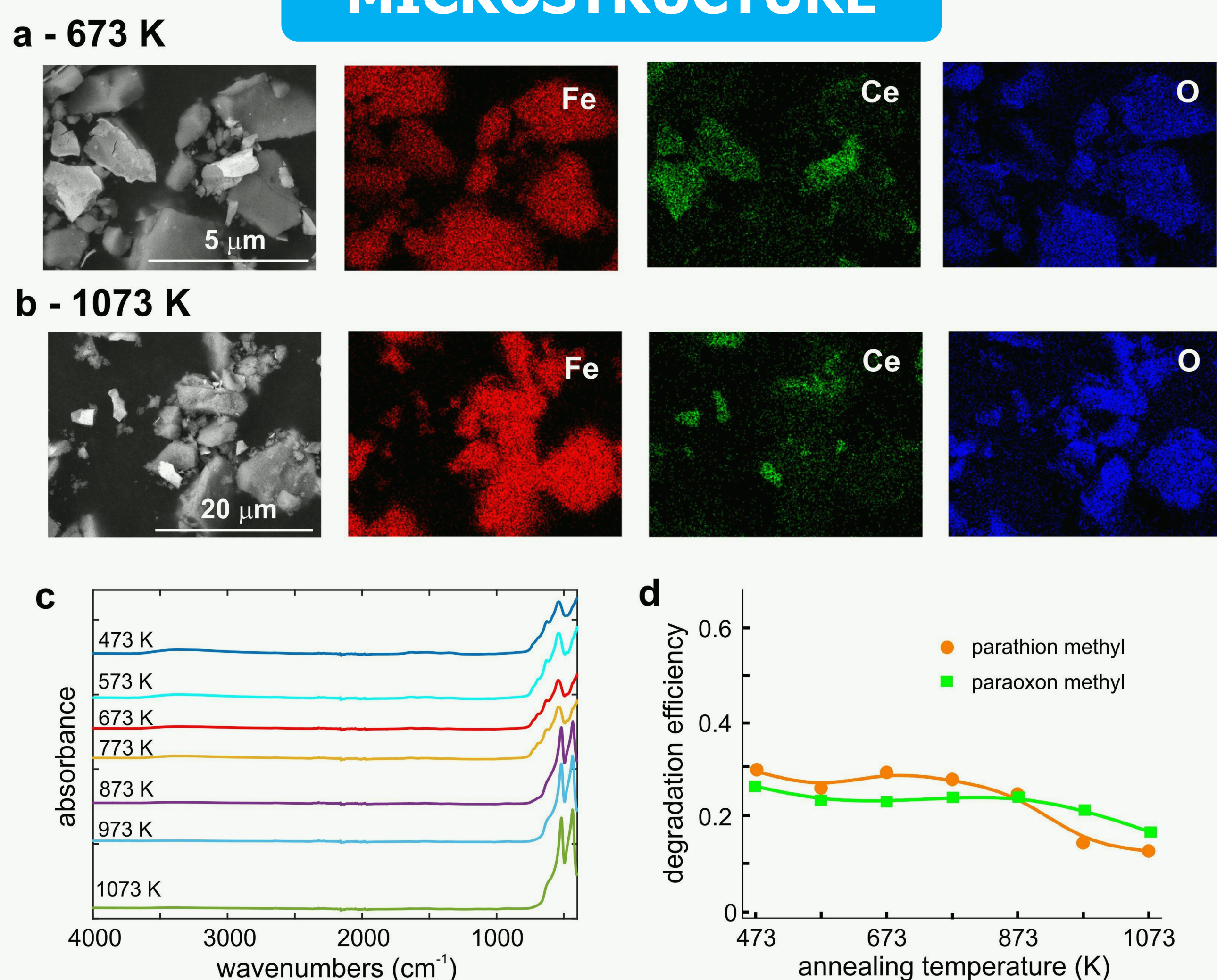
SAMPLE PREPARATION

- Magnetically separable sorbent** – composite material consisting of iron oxide serving as a magnetically separable core or carrier and cerium dioxide (CeO₂) serving as active constituent capable to destroy dangerous chemicals
- Magnetite core** – synthesized by the co-precipitation of the Fe²⁺ (ferrous sulphate monohydrate) and Fe³⁺ (ferric sulphate) salts from cheap and commercially available raw materials
- CeO₂/Fe-oxide reactive sorbents**
 - ferrimagnetic core re-dispersed in the solution containing 5 wt.% of cerium (III) nitrate, and the cerium (III) carbonate prepared by precipitation with ammonium hydrogen carbonate
 - finally cerous carbonate/magnetite precursor annealed (calcined) in a muffle furnace at various temperatures T_a ranging from 473 to 1073 K for 2h
- Testing the effectiveness of sorbents** – using the pesticides parathion methyl in an aprotic environment and paraoxon methyl in an aqueous environment

EXPERIMENTAL TECHNIQUES

- XRD (X-Ray Diffraction)** – X'PERT PRO diffractometer (Panalytical) equipped with Co K α radiation ($\lambda = 0.17902$ nm), 2θ range 20° - 135°, evaluation – Rietveld structure refinement method by using the HighScore Plus program and the ICSD database
- SEM (Scanning Electron Microscopy)** – TESCAN LYRA 3XMU FEG/SEM, accelerating voltage 20 kV, equipped with an X-Max80 Oxford Instruments energy-dispersive X-ray (EDX) detector
- FTIR (Fourier Transform InfraRed) spectroscopy** – Nicolet iS50 (Thermo Scientific), single ATR mode on diamond crystal (32 scans, 4 cm⁻¹ resolution), range of wavelengths 2.5 - 25 μ m
- VSM (Vibrating-Sample Magnetometer)** – Microsense EZ9, room temperature (RT) magnetization and virgin curves - maximal magnetic field 1600 kA/m, first-order reversal curves (FORC) with step 8 kA/m
- PPMS (Physical Property Measurement System)** – Quantum design, Inc., field-cooled (FC) and zero-field-cooled (ZFC) curves in the temperature range 2-293 K in magnetic field of 8 kA/m

MICROSTRUCTURE



(a,b) SEM images and EDX distribution maps of Fe, Ce, and O of samples annealed at 673 K and 1073 K. FTIR spectra (c) and degradation efficiency against parathion and paraoxon methyl (d) depicted in dependence on annealing temperature.

The results of Rietveld analysis of sorbents annealed at T_a temperature; phase content (A), lattice parameters (a , b , c), microdomain size (d).

T_a (K)	CeO ₂			Fe ₃ O ₄			γ -Fe ₂ O ₃				α -Fe ₂ O ₃			
	A (%)	$a = b = c$ (nm)	d (nm)	A (%)	$a = b = c$ (nm)	d (nm)	A (%)	$a = b$ (nm)	c (nm)	d (nm)	A (%)	$a = b$ (nm)	c (nm)	d (nm)
473	5.4	0.5394	3.2	42.9	0.8368	8.3	51.7	0.8341	0.8299	11.8	-	-	-	-
573	4.8	0.5413	3.4	28.4	0.8333	11.7	66.8	0.8391	0.8258	8.3	-	-	-	-
673	5.3	0.5411	6.4	32.5	0.8331	14.6	62.2	0.8402	0.8247	8.7	-	-	-	-
773	5.0	0.5408	8.4	25.7	0.8383	7.8	61.6	0.8329	0.8322	11.3	7.7	0.5031	1.3736	40.3
873	4.2	0.5408	10.4	-	-	-	3.3	0.8368	0.8323	11.5	92.5	0.5034	1.3751	41.9
973	4.6	0.5408	12.3	-	-	-	-	-	-	-	95.4	0.5034	1.3747	47.4
1073	4.7	0.5409	14.0	-	-	-	-	-	-	-	95.3	0.5035	1.3748	51.3

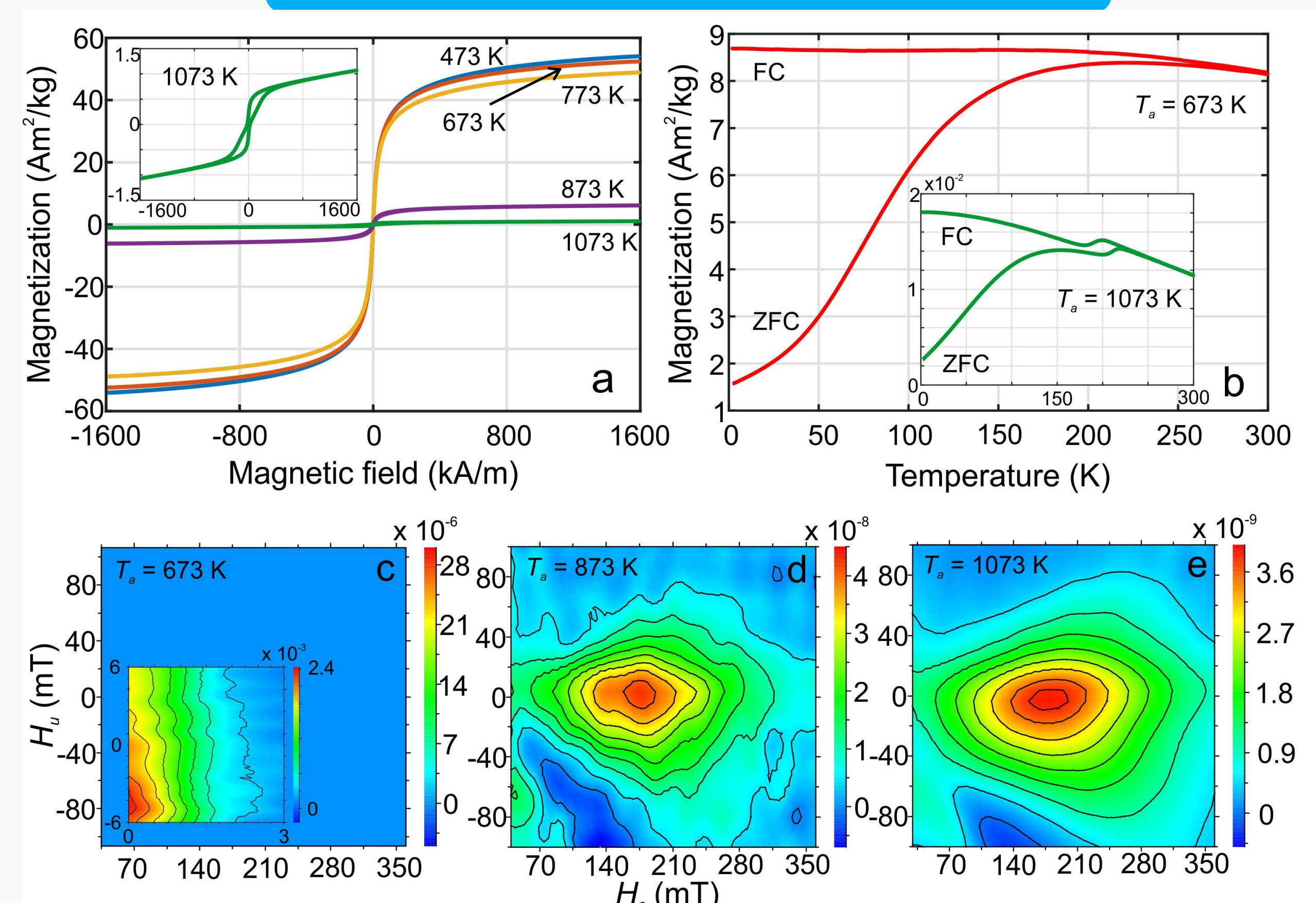
• **SEM and EDX analysis** indicate that the powders contain a mix of grains of different sizes, some are enriched in Ce, others are Ce depleted.

• **XRD results** show that transformation of magnetite and maghemite to hematite starts at 773 K and finishes at 973 K, microdomain size of CeO₂ and hematite gradually grows with increasing T_a .

• **FTIR spectra** – sorbents annealed at 873 K – 1073 K show two peaks at 518 cm⁻¹ and 436 cm⁻¹ characteristic for stretching vibrations of Fe-O bond in hematite, sorbents annealed below 873 K exhibit one peak moved to 540 cm⁻¹ reflecting magnetite (maghemite), vibrations Ce-O (about 520 cm⁻¹) were not conclusively confirmed by FTIR.

• **Degradation efficiency** – about 30% for sorbents with 5 wt.% CeO₂ annealed at 473 K – 773K, it could be increased by adding higher content of cerium dioxide.

MAGNETIC PROPERTIES



(a) Magnetization curves measured at different annealing T_a temperatures. (b) ZFC-FC curves of samples annealed at 673 K and 1073 K (inset). First-order reversal curves (FORC) of sorbents annealed at (c) 673 K, (d) 873 K, and (e) 1073 K.

RT magnetic properties obtained from hysteresis loops and Henkel plots in dependence on annealing T_a temperature; magnetization at magnetic field 1600 kA/m (M_{1600}), remanent magnetization (M_r), coercive field (H_c), position of peak (ΔM , ΔH) from the Henkel plots.

T_a (K)	M_{1600} (Am ² /kg)	M_r (Am ² /kg)	H_c (kA/m)	ΔM (Am ² /kg)	ΔH (kA/m)
473	54.09	0.32	0.23	0.07	25.02
573	52.95	0.29	0.21	0.05	25.14
673	52.42	0.30	0.22	0.06	25.18
773	48.85	0.23	0.18	0.06	25.22
873	6.14	0.19	1.07	0.04	180.16
973	1.14	0.20	18.25	0.03	203.72
1073	1.07	0.20	21.53	0.03	203.95

• RT hysteresis loops detect predominantly **strong iron oxide responses**, which are several orders of magnitude higher than that of cerium dioxide.

• **Sorbents annealed at 473 K – 773 K:** low H_c and high M_{1600} at RT, blocking and irreversible temperatures about 220 K and 256 K, increase of H_c and M_r after cooling to 2 K.

• **Sorbents annealed at 873 K – 1073 K:** increase of H_c and decrease of M_{1600} at RT due to main hematite contribution, hysteresis loops consist of ferromagnetic reversal followed by the linear increase of magnetization corresponding to antiferromagnetic order, Morin transition about 200 K.

• **Henkel plots** – obtained from virgin and hysteresis loops at RT, convex curves showing negative (dipolar) magnetic interactions for all samples, the strongest interactions observed at the peak position ΔH , ΔM (see table), marked increase of ΔH after annealing at 873 K.

• **FORC diagrams** – map of the magnetic response of all particles in a sample with irreversible magnetizations in terms of the coercivity (switching field) $H_c = H_{sw}$ and magnetic interaction field $H_u = H_{int}$ distribution, the maximum close to zero (sample 673 K) indicates the presence of magnetite and maghemite, clear contours with one central peak correspond to the dominance of the hematite (samples 873 K and 1073 K), H_c is very close to the ΔH of the Henkel plot.